

## NOTES

## TEM Analysis of Pillared and Delaminated Hectorite Catalysts\*

When a dispersion of clay particles flocculates in water, the plates may associate as face-to-face (FF), edge-to-edge (EE), or edge-to-face (EF) (1). The FF association forms thicker particles whereas EF and EE interactions generate large three-dimensional aggregates which Van Olphen described as having a house-of-card structure (1). These two modes of particle association can be observed also in solids. In fact, by ion-exchanging the charge compensating cations in layer-lattice clay minerals such as montmorillonite or hectorite with large organic (2) or inorganic cations, multi-layered FF aggregates are formed; these materials, called pillared clays, have been reviewed by Pinnavaia (3). Clay particle aggregates containing EF and EE linkages are called delaminated clays (4).

Delaminated clays are a new family of catalysts first prepared by Pinnavaia and co-workers (4, 5) by reacting a synthetic hectorite with polyoxocations of aluminum in a manner described in the references given (4, 5). In these materials, 001 X-ray reflections are absent due to a lack of long range FF stacking of the clay silicate layers. Short range FF layer ordering is believed to be responsible for the zeolite-like selectivity in cracking gas oil (6). Delaminated clays are characterized by EE and EF connections which form a macrospace of the type found in amorphous aluminosilicate supports (7).

In contrast, pillared clays, are characterized by regularly spaced FF layers of clay platelets propped apart by inorganic oxide clusters. Tokarz and Shabtai (8) have

shown transmission electron micrographs (TEM) of  $Ce^{+3}$ -montmorillonite before and after pillaring. It is the purpose of this note to present TEM and electron diffraction data that will further characterize the structure of delaminated clay catalysts.

A 30-g sample of natural hectorite (obtained from the industrial division of N L Industry) was slurried in 4 liters of distilled water and reacted with an excess (70 g) of Chlorhydrol (an hydroxyaluminum oligomer from the Reheis Chemical Company) at  $pH \approx 5.0$ . The washed, air-dried, and calcined ( $500^{\circ}C/10$  hr in air) pillared hectorite catalyst had a basal spacing of  $14.9 \text{ \AA}$  and  $250 \text{ m}^2/\text{g}$  BET surface area. Pillared hectorite catalysts have been described in detail elsewhere (9).

The delaminated clay catalyst was prepared using Laponite-B, a synthetic fluorohectorite from Laporte Industries. This synthetic smectite forms thixotropic gels in water and typically contains 56.1%  $SiO_2$ , 26.6%  $MgO$ , 1.4%  $Li_2O$ , 3.6%  $Na_2O$  with 5.6% F and has  $380 \text{ m}^2/\text{g}$  BET surface area. A slurry was formed by adding 30 g of Laponite-B to 4 liters of distilled water; after addition of 70 g of Chlorhydrol, the gel formed was washed until chloride free, and then reslurried in 2 liters of distilled water. The washed gel was immersed in an ice-NaCl bath and freeze-dried in vacuo with a Buchi rotavapor. The clay thus prepared was found to be X-ray amorphous; its surface area had increased to  $420 \text{ m}^2/\text{g}$ , and, its cracking activity for gas oil conversion increased to 2.3 from 0.43 in the parent laponite (10).

TEM observation was carried out using a JEOL 100 CX microscope operating at 100 keV. Samples were dispersed by ultrasonic

\* Based in part on a paper presented at the Sixth Roermond Conference on Catalysis, Roermond, The Netherlands, July 1986.

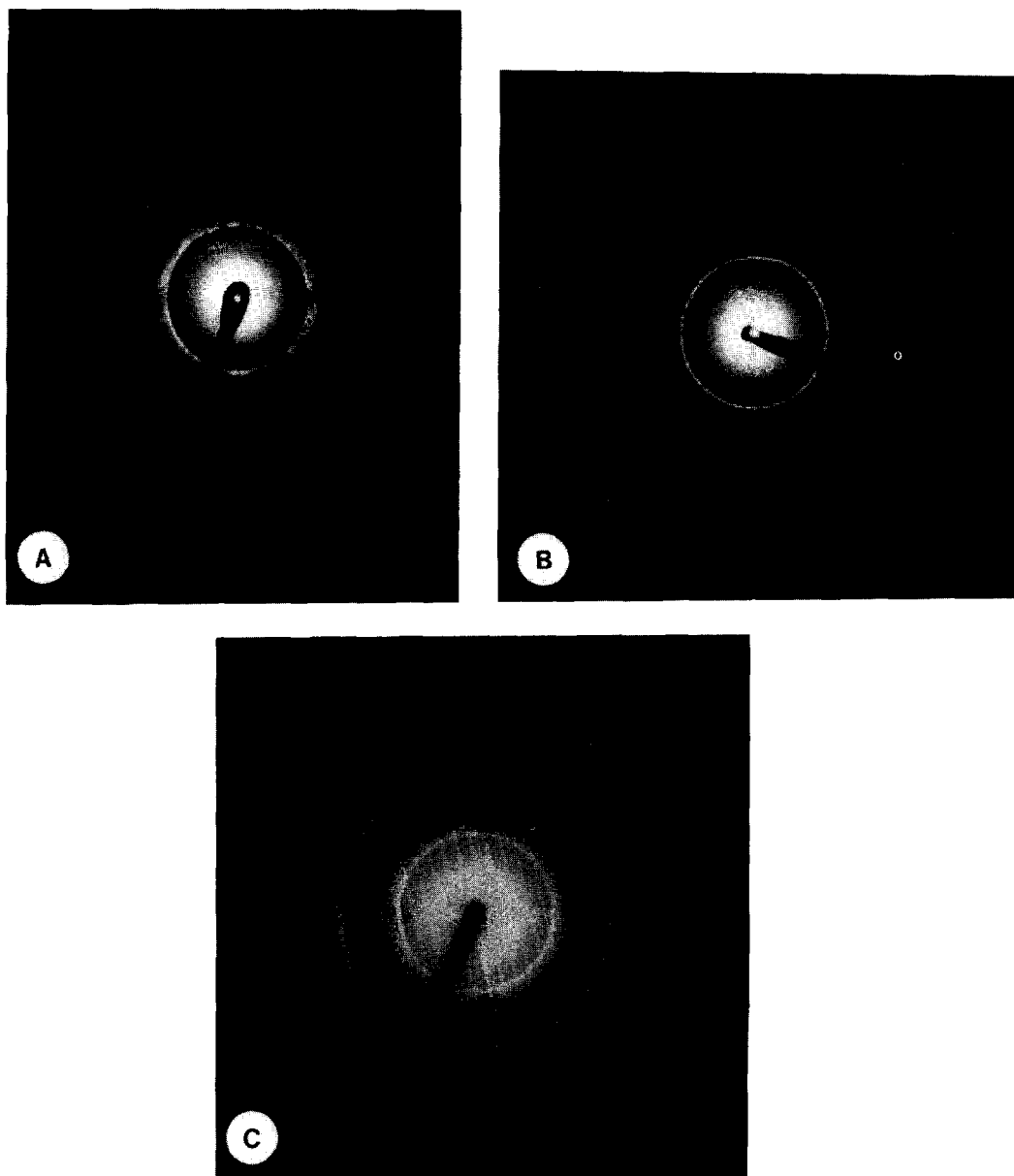


FIG. 1. Electron diffraction patterns of (A) montmorillonite, (B) natural hectorite, (C) pillared hectorite, (D) synthetic hectorite (laponite-B), and (E) delaminated laponite catalyst.

agitation in ethanol or water. A drop of the suspension was allowed to dry on a holey carbon film. Micrographs were obtained from parts of the specimen over holes in the film to avoid contrast from the amorphous carbon.

Electron diffraction patterns can be obtained from all of the clay catalysts under

study. Examples are given in Fig. 1. A well ordered clay with mainly FF contacts, such as montmorillonite (10) and (natural) hectorite gives a pattern dominated by  $hko$  reflexions because the plates are mostly lying flat on the support, normal to the electron beam (Figs. 1A and 1B). However, they are thin, and buckled or tilted at all

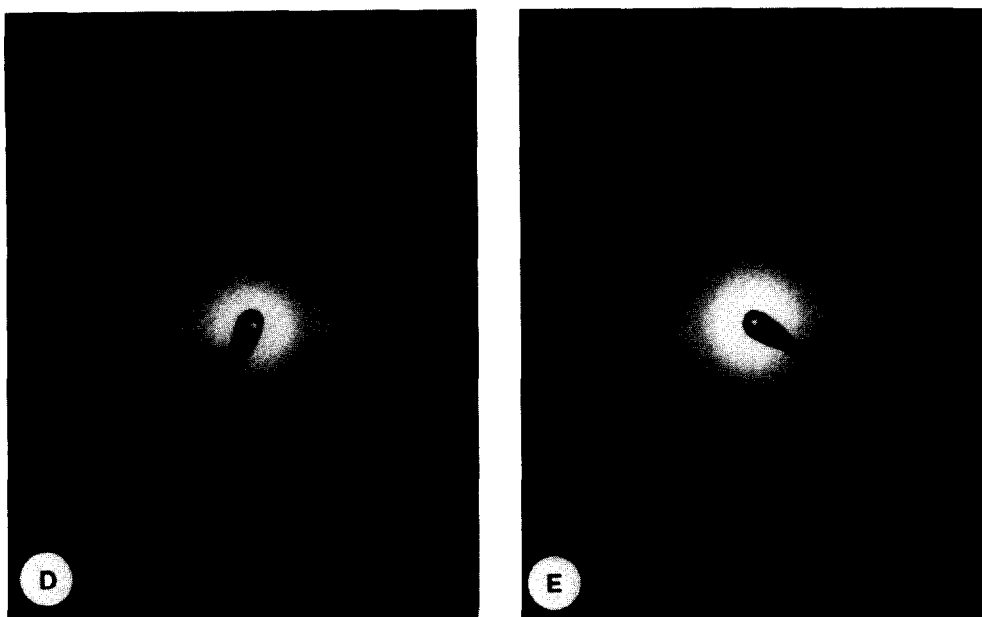


FIG. 1—Continued.

angles so that the rings of the powder pattern are sharp at the inner edge and diffuse at the outer edge. Reaction of (natural) hectorite with Chlorhydrol (9) cause the charge compensating Na ions to be replaced by the bulky hydroxyaluminum ions without affecting the long range FF stacking of the silicate layers. The diffusions of the outer edges of the diffraction rings is marked in the pillared hectorite but it is not evident in the parent material (Figs. 1B and 1C); this difference is consistent with an increase in the average distance between the silicate layers due to pillaring. However, like pillared bentonite (11), the pillared hectorite could not sorb perfluorotributylamine,  $[\text{CF}_3(\text{CF}_2)_3]_3\text{N}$ , a molecule with a kinetic diameter of about 10 Å.

Synthetic hectorite (Laponite-B) also gives *hko* reflections out to quite high orders (more than 060) indicating that the structure is well ordered within the sheets (Fig. 1D). As for Figs. 1A and 1B, and for the same reason, these rings are sharp on the inner and diffuse on the outer edge. These *hko* reflections are, in general, less

intense, probably because of stacking disorders. The spacings of these *hko* rings correspond to the lattice spacings for hectorite given in ASTM 9-31. In addition, there are diffuse reflections (arrows in Fig. 1D) corresponding to spacings of about 9.84, 4.92 and 3.20 Å which must be the *ool* reflections for  $l = 1, 2, 3$ . These reflections, unlike the *hko* rings, are symmetrically diffuse. In the pattern in Fig. 1D, all the reflexions are arced because of preferred orientation in the area selected.

After reaction with polyoxocations of aluminum (Chlorhydrol) and freeze-drying, the laponite catalyst contains 24.5%  $\text{Al}_2\text{O}_3$  and its  $\text{Na}_2\text{O}$  level is reduced from 3.55% to about 0.15%. In contrast to pillared clays, this catalyst can sorb 17–22 wt% perfluorotributylamine at 25°C. The delaminated hectorite gives a pattern similar to that of the parent synthetic hectorite but with the *ool* reflexions consistently less intense (see Fig. 1E) because of increased stacking disorders.

Typical transmission electron micrographs of the parent hectorite together with

the pillared and delaminated hectorite catalysts are shown in Figs. 2-5. The synthetic fluoro-hectorites' (laponite-B) morphology is very different from that of the natural

clay. In contrast to montmorillonites and natural hectorites, long range FF stacking is absent. Blocks of platelets and FE and EF connections appear to be the main

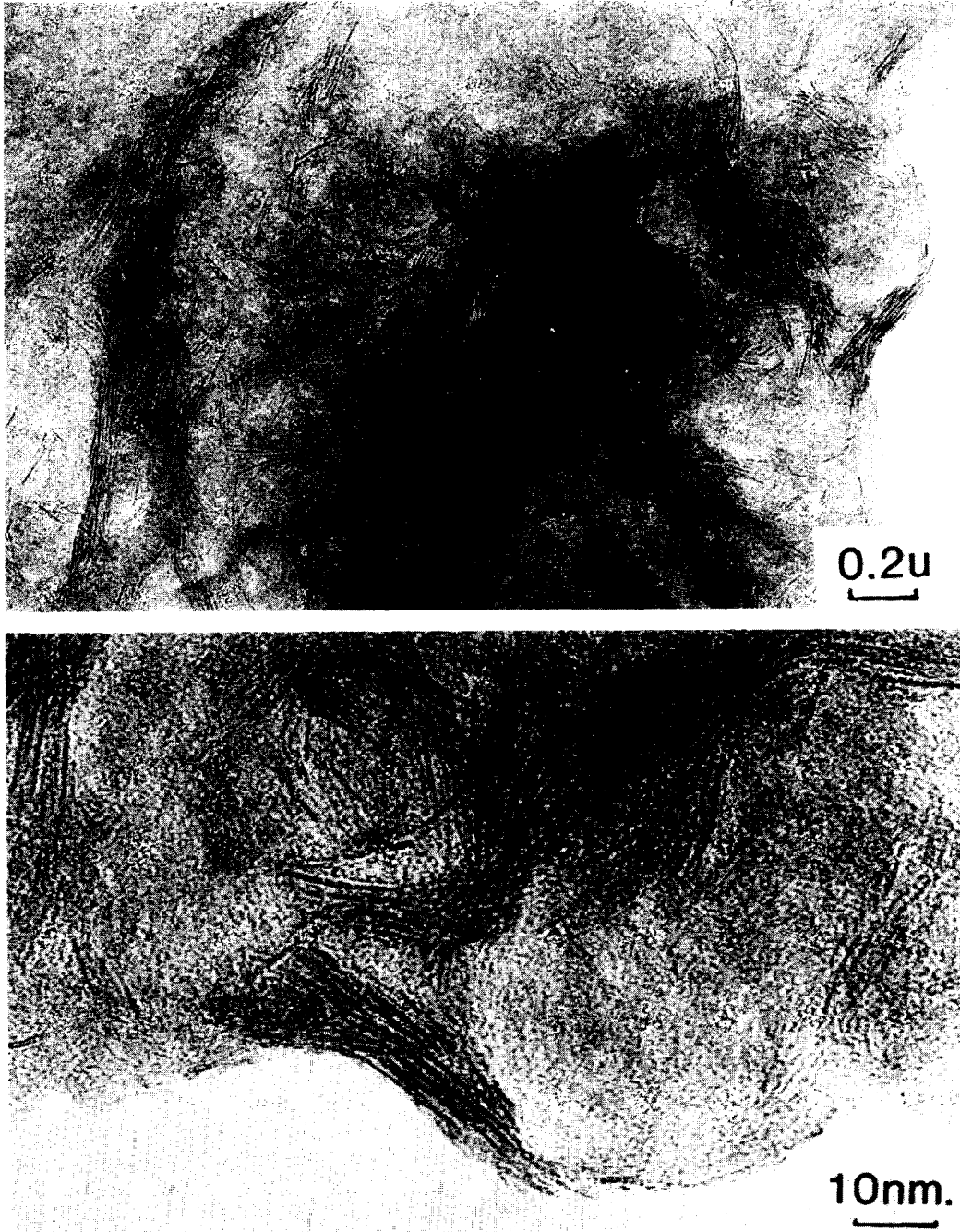


FIG. 2. TEM micrographs of the parent synthetic hectorite (Laponite-B).

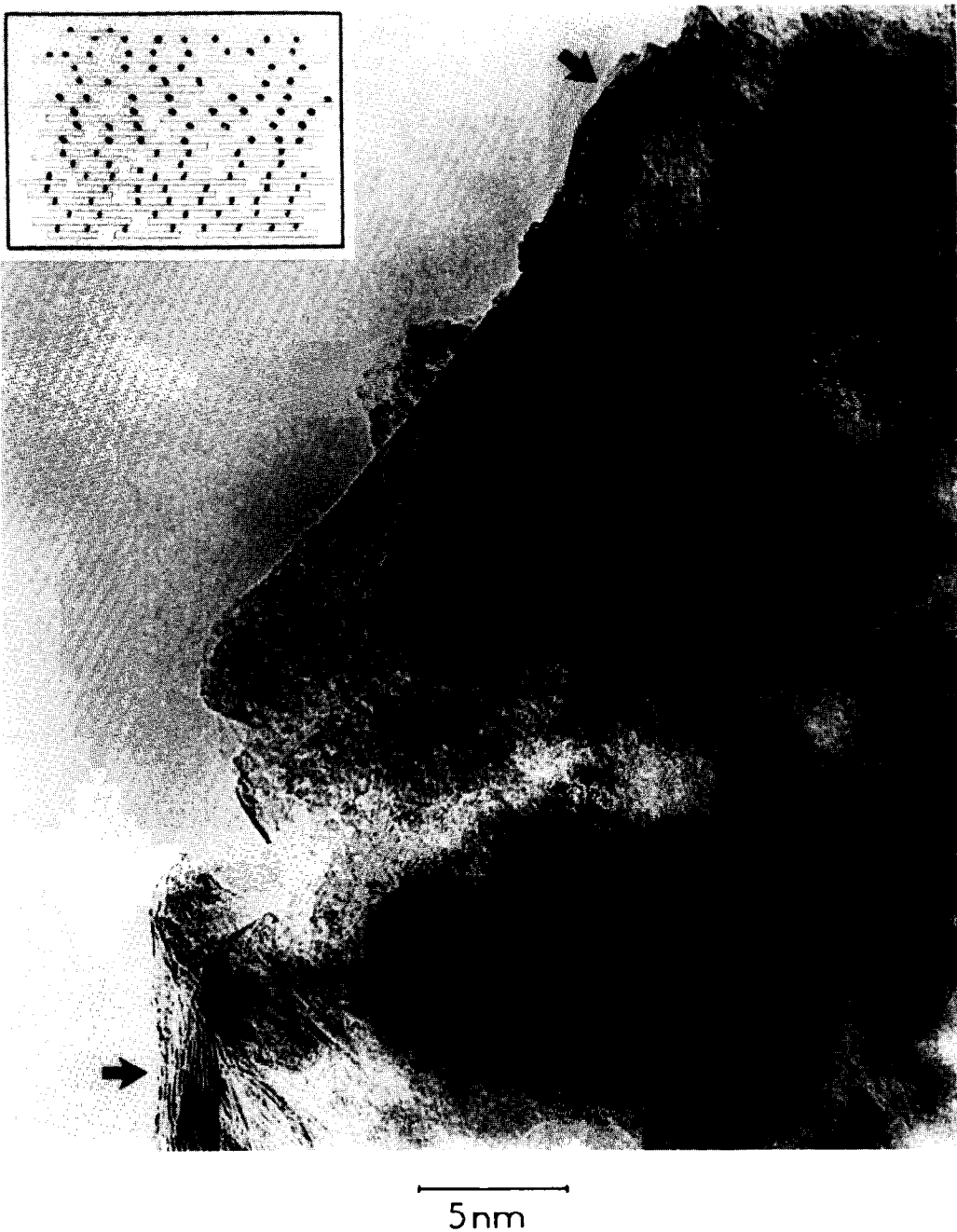


FIG. 3. TEM micrographs of pillared hectorite. The pointing arrows show the ordered face-to-face layer stacking, the insert illustrates the schematic representation of the pillared structure.

mode of plate aggregation. Furthermore, crystals are highly disorganized and individual sheets (about one basal plane thick) can be seen (Fig. 2). Both natural and

synthetic hectorites consist of large sheets slightly buckled at the edges where basal planes can be seen; the buckling is somewhat more pronounced in the pillared than

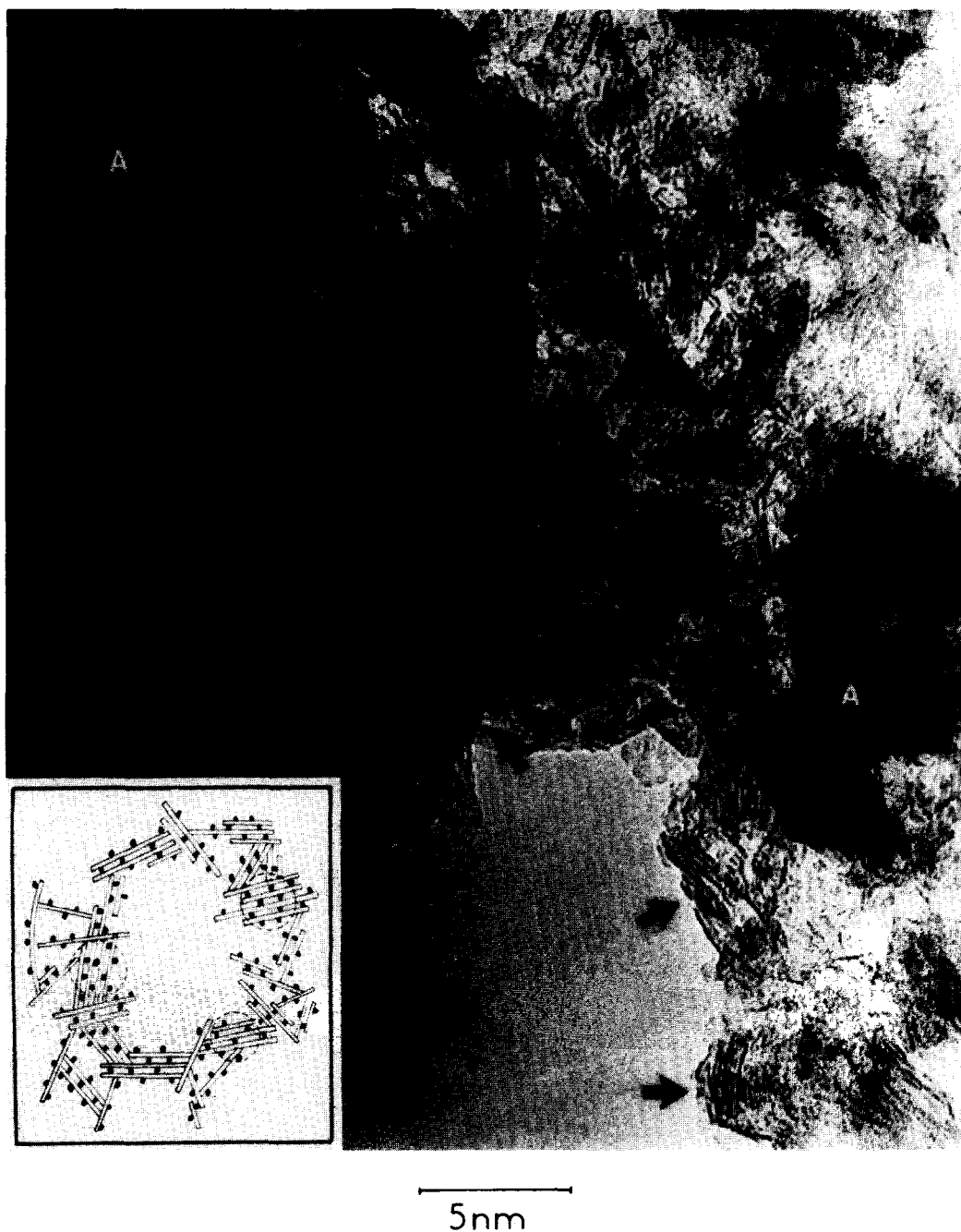


FIG. 4. TEM micrograph of a delaminated laponite. Some poorly crystallized alumina is sometimes present (A). The pointing arrows show the distribution of unit layer aggregates (dotted circles in the insert), the building blocks of the house-of-card structure.

in the parent hectorite. This twisting of the sheets makes it difficult to obtain an accurate lattice parameter by TEM; the interpla-

nar spacings appear to be about 11 Å constantly smaller than those obtained by X-ray diffraction measurements. In fact,

the X-ray diffractograms in Fig. 6 clearly show an increase in the natural hectorite basal plane spacing from  $\sim 12$  to  $14.9 \text{ \AA}$  upon pillaring and calcination whereas little expansion is observable in TEM. This discrepancy is attributed to dehydration of



FIG. 5. Additional TEM micrograph of a delaminated laponite showing the distribution of aggregates containing about 4 to 8 unit layers held together by face-to-face connections. Some poorly crystallized alumina is also present (A).

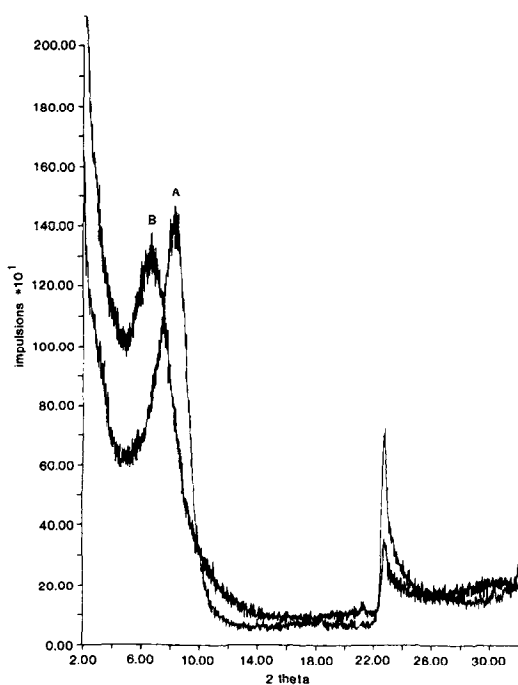


FIG. 6. X-ray diffractograms of natural hectorite (A) before and (B) after pillaring with Chlorhydrol and calcination in air at 400°C/10 h.

specimens in the vacuum chamber of the microscope. The pillared material exhibits unit layers parallel to each other propped apart by about  $\sim 8\text{--}10 \text{ \AA}$ , to be compared with a basal spacing of about  $14.9 \text{ \AA}$  measured by X-ray diffraction and with a well ordered FF unit layer stacking as shown in the insert in Fig. 3. Although some dislocations are present, the continuity of the basal planes may extend over several hundred angstroms.

Figures 4 and 5 show the existence of a mode of particle distribution characterized by aggregates containing about 4 to 8 unit layers held together by FF association (corresponding to the dotted circles in Fig. 4 insert). It is believed that EF (and to a lesser extent, EE) connections between these well dispersed aggregates form a three-dimensional structure which extends throughout the clay catalyst. Differences in morphology (and particle sizes) is thought to be the main cause of the different modes of particle aggregation observed in these

(natural and synthetic) clay minerals (see Figs. 3–5). Some poorly crystallized alumina forms during calcination in air of the delaminated catalyst (Figs. 4 and 5). A high performance acquisition system (Tracor Northern 5700) was installed on the STEM to generate elemental maps of the pillared and delaminated catalysts. These efforts were unsuccessful because of sample instability.

In summary, the macrospace of a delaminated clay catalyst is probably a three-dimensional network of 4 to 8 unit layer aggregates linked together mainly by FE (and EE) interactions. There is some FF plate association, forming aggregates which contain the microporosity of pillared clays and zeolites. The aggregates are held together by crosslinked particles forming a stable house-of-card structure with macroporosity usually found in silicas, aluminas, and mixed oxide catalysts. The delaminated clay macropores allow the sorption of large molecules such as perfluorotributylamine which cannot be sorbed in pillared clay catalysts.

#### REFERENCES

1. Van Olphen, H., "An Introduction to Clay Colloid Chemistry," 2nd ed., p. 43. Wiley, New York, 1977.
2. Barrer, R. M., "Zeolites and Clay Minerals as Sorbents and Molecular Sieves." Academic Press, New York, 1978.
3. Pinnavaia, T. J., *Science* **220**, 4595 (1983).
4. Pinnavaia, T. J., "Heterogeneous Catalysis" (B. L. Shapiro, Ed.), p. 142. Texas A&M Univ. Press, College Station, TX, 1984.
5. Pinnavaia, T. J., Tzou, M. S., Landau, S. D., and Raythathe, R. H., *J. Mol. Catal.* **27**, 195 (1984).
6. Occelli, M. L., Landau, S. D., and Pinnavaia, T. J., *J. Catal.* **90**, 256 (1984).
7. Occelli, M. L., Landau, S. D., and Pinnavaia, T. J., *J. Catal.* (1987, in press).
8. Shabtai, J., Rosell, M., and Tokarz, M., *Clays Clay Miner.* **32**, 99 (1984).
9. Occelli, M. L., and Finseth, D. H., *J. Catal.* **49**, 316 (1986).
10. Occelli, M. L., *J. Mol. Catal.* **35**, 377 (1986).
11. Vaughan, D. E. W., and Lussier, R. J., in "Proc. 5th Int. Conf. Zeolites" (L. V. Rees, Ed.), p. 24. Hyden, London, 1980.



M. L. OCCELLI

J. V. SENDERS

*Unocal Science & Technology Division  
Brea, California 92621*

*CSIRO Division of Material Science  
Locked Bag 33  
Clayton, Victoria  
Australia*

J. LYNCH

*Institut Francais du Petrole, B.P. 311  
92506 Rueil-Malmaison Cedex  
France*

*Received March 23, 1986*